Structure, Vol. 10, 743–749, June, 2002, PII S0969-2126(02)00786-4

Paper Alert

A selection of interesting papers that were published in the month before our press date in major journals most likely to report significant results in structural biology, protein, and RNA folding.

□ **Conformational flexibility of bacterial RNA polymerase.** Seth A. Darst, Natacha Opalka, Pablo Chacon, Andrey Polyakov, Catherine Richter, Gongyi Zhang, and Willy Wriggers (2002). Proc. Natl. Acad. Sci. USA *99*, 4296–4301.

cEM and image processing of helical crystals has been used to determine the structure of *Escherichia coli* core RNA polymerase (RNAP) to a nominal resolution of 15 Å. The authors made use of a recently described method for averaging Fourier-Bessel coefficients (D. DeRosier, D.L. Stokes, and S.A. Darst [1998]. J. Mol. Biol. *289*, 159–165) to generate an averaged map that combined data from four different helical symmetries. The high conservation of the sequence of the core RNAP subunits allowed the use of the high resolution Thermus aquaticus core RNAP structure in the interpretation of the cEM-derived density. A close correspondence was seen between the two structures with the major differences ascribed to deletions or insertions between the Taq and *E. coli* RNAPs. Despite this similarity, a large conformation change was required to fit the Taq structure to the *E. coli* one. The authors suggest that this large conformation change reflects the normal flexibility of the RNAP. The conformational change is dominated by a nearly 20° hinge-like rotation while the core region of the structure remains relatively intact.

□ **Quaternary structure of human fatty acid synthase by electron cryomicroscopy.** Jacob Brink, Steven J. Ludtke, Chao-Yuh Yang, Zei-Wei Gu, Salih J. Wakil, and Wah Chiu (2002). Proc. Natl. Acad. Sci. USA *99*, 138–143.

The authors employed a combination of cEM and single particle image reconstruction to determine the structure of human fatty acid synthase (FAS) (M_r 272,000) to a resolution of 19 Å. Low angle X-ray scattering was used to define the profile and control the correction of the contrast transfer function. The reconstruction imposed C2 symmetry; processing without imposing symmetry produced a noisier structure with a resolution of 23 Å. The authors conclude that the molecule must have approximate C2 symmetry but that a larger, higher signal-to-noise data set would necessary to demonstrate the symmetry conclusively. The two anti-parallel monomers in the complex each show three domains. The authors suggest the active sites are formed by juxtaposition of half sites in the dimer.

□ **Structure of the cell-puncturing device of bacteriophage T4.** Shuji Kanamaru, Petr G. Leiman, Victor A. Kostyuchenko, Paul R. Chipman, Vadim V. Mesyanzhinov, Fumio Arisaka, and Michael G. Rossmann (2002). Nature *415*, 553–557.

Bacteriophage T4 penetrates the cell and initiates infection by means of interactions with its baseplate. This structure, located at the end of the phage tail, regulates the interaction of the tail fibers and the DNA ejection machine. The central part of the baseplate is a complex of gp5 (63K) and gp27 (44K), which is required to penetrate the outer cell membrane and to disrupt the peptidoglycan layer. The authors present the structure of the $(gp5–gp27)_3$ 321K complex, determined to 2.9 Å resolution by X-ray crystallography. They also determined the context for this high resolution structure by fitting into the structure of baseplate-tail tube assembly determined to 17 Å resolution by cEM. The gp27 cylinder is an extension of the tail tube which is continued by the three N-terminal domains of gp5. The diameter of the gp27 cylinder could accommodate the dsDNA helix and form the channel for penetration.

□ **A 11.5 Å single particle reconstruction of GroEL using EMAN.** Steven J. Ludtke, Joanita Jakana, Jiu-Liu Song, David T. Chuang, and Wah Chiu (2001). J. Mol. Biol. *314*, 253–262.

cEM and single particle reconstruction of GroEL, was performed using EMAN, a single-particle analysis software package, to generate a three-dimensional reconstruction to approximately 11.5 A. The authors demonstrate that the single-particle reconstruction, X-ray scattering data and X-ray crystal structure all agree well at this resolution.

□ **Striking conformational change suspected within the phosphoribulokinase dimer induced by its interaction with GAPDH.** Fabrice Mouche, Brigitte Gontero, Isabelle Callebaut, Jean-Paul Mornon, and Nicolas Boisset (2002). J. Biol. Chem. *277*, 6743–6749.

Many enzymes are found as multi-enzyme complexes in the cell. Some of these complexes are believed to enhance enzyme activity by channeling substrates between consecutive steps of a pathway. Others are believe to modulate the activities of the intrinsic properties of the enzyme within the complex. The authors combined cEM and image reconstruction with comparison with high resolution structures of homologous enzymes to study the $(\text{glyceraldehyde-3-phosphate dehydrogenase (GAPDH)})_{2\times4}$ – $(\text{phosphoribulokinase(PRK)})_{2\times2}$ complex. The authors determined the structure of the complex to 29.5 Å from cEM. Fitting of the high-resolution structures of isolated PRK and GAPDH into the reconstruction defined their positions and showed that their conformations were altered in the complex.

□ **Structure of the HP1 chromodomain bound to histone H3 methylated at lysine 9.** Peter R. Nielsen,

Daniel Nietlispach, Helen R. Mott, Juliana Callaghan, Andrew Bannister, Tony Kouzarides, Alexey G. Murzin, Natalia V. Murzina, and Ernest D. Laue (2002). Nature *416*, 103–107.

Specific modifications to histones are heritable changes in gene expression that do not affect the DNA sequence. Methylation of lysine 9 in histone H3 is recognized by heterochromatin protein 1 (HP1), which directs the binding of other proteins to control chromatin structure and gene expression. Here the authors show that HP1 uses an induced-fit mechanism for recognition of this modification, as revealed by the structure of its chromodomain bound to a histone H3 peptide dimethylated at N of lysine 9. The binding pocket for the N-methyl groups is provided by three aromatic side chains that become ordered on binding of the peptide. The QTAR peptide sequence preceding Lys 9 makes most of the additional interactions with the chromodomain, leading the authors to predict which other chromodomains will bind methylated proteins.

□ **Crystal structure of DegP (HtrA) reveals a new protease-chaperone machine**. Tobias Krojer, Marta Garrido-Franco, Robert Huber, Michael Ehrmann, and Tim Clausen (2002). Nature *416*, 455–459.

Molecular chaperones and proteases monitor the folded state of other proteins. In addition to recognizing nonnative conformations, they distinguish substrates that can be refolded from those that need to be degraded. DegP (also known as HtrA) is a conserved heat shock protein that combines refolding and proteolytic activities. The crystal structure of the DegP hexamer reveals a staggered association of trimeric rings. The proteolytic sites are located in a central cavity that is only accessible laterally. The mobile side-walls are constructed by twelve PDZ domains, which mediate the opening and closing of the particle and probably the initial binding of substrate. The inner cavity is lined by several hydrophobic patches that may act as docking sites for unfolded polypeptides. In the chaperone conformation, the protease domain of DegP exists in an inactive state, in which substrate binding in addition to catalysis is abolished.

□ **The crystal structure of class II ribonucleotide reductase reveals how an allosterically regulated monomer mimics a dimer**. Michael D. Sintchak, Gitrada Arjara, Brenda A. Kellogg, JoAnne Stubbe, and Catherine L. Drennan (2002). Nat. Struct. Biol. *9*, 293–300.

Ribonucleotide reductases (RNRs) catalyze the conversion of ribonucleotides to deoxyribonucleotides, an essential step in DNA biosynthesis and repair. The authors present the crystal structure of class II (coenzyme B12-dependent) ribonucleoside triphosphate reductase (RTPR) from *Lactobacillus leichmannii* in the apo enzyme form and in complex with the B12 analog adeninylpentylcobalamin at 1.75 and 2.0 Å resolution, respectively. This monomeric, allosterically regulated class II RNR retains all the key structural features associated with the catalytic and regulatory machinery of oligomeric RNRs. Surprisingly, the dimer interface responsible for effector binding in class I RNR is preserved through a single 130-residue insertion in the class II structure. Thus, *L. leichmannii* RNR is a paradigm for the simplest structural entity capable of ribonucleotide reduction, a reaction linking the RNA and DNA worlds.

□ **A pre-translocational intermediate in protein synthesis observed in crystals of enzymatically active 50S subunits**. T. Martin Schmeing, Amy C. Seila, Jeffrey L. Hansen, Betty Freeborn, Juliane K. Soukup, Stephen A. Scaringe, and Scott A. Strobel, Peter B. Moore, and Thomas A. Steitz (2002). Nat. Struct. Biol. *9*, 225–230.

The authors describe a version of the large ribosomal subunit peptidyl transferase activity assay that does not require alcohol and use it to show, both crystallographically and biochemically, that crystals of the large ribosomal subunits from *Haloarcula marismortui* are enzymatically active. Addition of these crystals to solutions containing substrates results in formation of products, which ceases when crystals are removed. When substrates are diffused into large subunit crystals, the subsequent structure shows that products have formed. The CC-puromycin-peptide product is found bound to the A-site and the deacylated CCA is bound to the P-site, with its 3′ OH near N3 A2486 (*Escherichia coli* A2451). Thus, this structure represents a state that occurs after peptide bond formation but before the hybrid state of protein synthesis.

□ **The PWWP domain of mammalian DNA methyltransferase Dnmt3b defines a new family of DNA binding folds**. Chen Qiu, Ken Sawada, Xing Zhang, and Xiaodong Cheng (2002). Nat. Struct. Biol. *9*, 217–224.

The PWWP domain is a weakly conserved sequence motif found in >60 eukaryotic proteins, including the mammalian DNA methyltransferases Dnmt3a and Dnmt3b. These proteins often contain other chromatin-association domains. A 135-residue PWWP domain from mouse Dnmt3b (amino acids 223–357) has been structurally characterized at 1.8 Å resolution. The N-terminal half of this domain resembles a barrel-like five-stranded structure, whereas the C-terminal half contains a five-helix bundle. The two halves are packed against each other to form a single structural module that exhibits a prominent positive electrostatic potential. The PWWP domain alone binds DNA in vitro, probably through its basic surface.

□ **Structure of the bacterial RNA polymerase promoter specificity subunit**. Elizabeth A. Campbell, Oriana Muzzin, Mark Chlenov, Jing L. Sun, C. Anders Olson, Oren Weinman, Michelle L. Trester-Zedlitz, and Seth A. Darst (2002). Mol. Cell *9*, 527–539.

The sigma subunit is the key regulator of bacterial tran-

scription. Proteolysis of *Thermus aquaticus* A, which occurred in situ during crystallization, reveals three domains, 2, 3, and 4, connected by flexible linkers. Crystal structures of each domain were determined, as well as of 4 complexed with -35 element DNA. Exposed surfaces of each domain are important for RNA polymerase binding. Universally conserved residues important for -10 element recognition and melting lie on one face of 2, while residues important for extended -10 recognition lie on 3; a helix-turn-helix motif in 4 recognizes the -35 element. Positive control mutants in 4 cluster in two regions, positioned to interact with activators bound just upstream or downstream of the -35 element.

□ **Crystal structure of the *Bacillus stearothermophilus* anti-factor SpoIIAB with the sporulation factor F.** Elizabeth A. Campbell, Shoko Masuda, Jing L. Sun, Oriana Muzzin, C. Anders Olson, Sheng Wang, and Seth A. Darst (2002). Cell *108*, 795–807.

Cell type-specific transcription during *Bacillus sporulation* is established by F. SpoIIAB is an anti- that binds and negatively regulates F, as well as a serine kinase that phosphorylates and inactivates the anti-anti-SpoIIAA. The crystal structure of F bound to the SpoIIAB dimer in the low-affinity, ADP form has been determined at 2.9 Å resolution. SpoIIAB adopts the GHKL superfamily fold of ATPases and histidine kinases. A domain of F contacts both SpoIIAB monomers, while 80% of the factor is disordered. The interaction occludes an RNA polymerase binding surface of F, explaining the SpoIIAB anti-activity. The structure also explains the specificity of SpoIIAB for its target factors.

□ **Structure of the C3b binding site of CR1 (CD35), the immune adherence receptor.** Brian O. Smith, Rosie L. Mallin, Malgorzata Krych-Goldberg, Xuefeng Wang, Richard E. Hauhart, Krystyna Bromek, Dusan Uhrin, John P. Atkinson, and Paul N. Barlow (2002). Cell *108*, 769–780.

Complement receptor type 1 (CR1 or CD35) is a multiple modular protein that mediates the immune adherence phenomenon, a fundamental event for destroying microbes and initiating an immunological response. It fulfills this role through binding C3b/C4b-opsonized foreign antigens. The structure of the principal C3b/C4b binding site (residues 901–1095) of CR1 is reported, revealing three complement control protein modules (modules 15–17) in an extended head-to-tail arrangement with flexibility at the 16-17 junction. Structure-guided mutagenesis identified a positively charged surface region on module 15 that is critical for C4b binding. This patch, together with basic side chains of module 16 exposed on the same face of CR1, is required for C3b binding. These studies reveal the initial structural details of one of the first receptor-ligand interactions to be identified in immunobiology.

□ **Structure of Dengue virus: implications for flavivirus organization, maturation, and fusion.** Richard J. Kuhn, Wei Zhang, Michael G. Rossmann, Sergei V. Pletnev, Jeroen Corver, Edith Lenches, Christopher T. Jones, Suchetana Mukhopadhyay, Paul R. Chipman, Ellen G. Strauss, Timothy S. Baker, and James H. Strauss (2002). Cell *108*, 717–725.

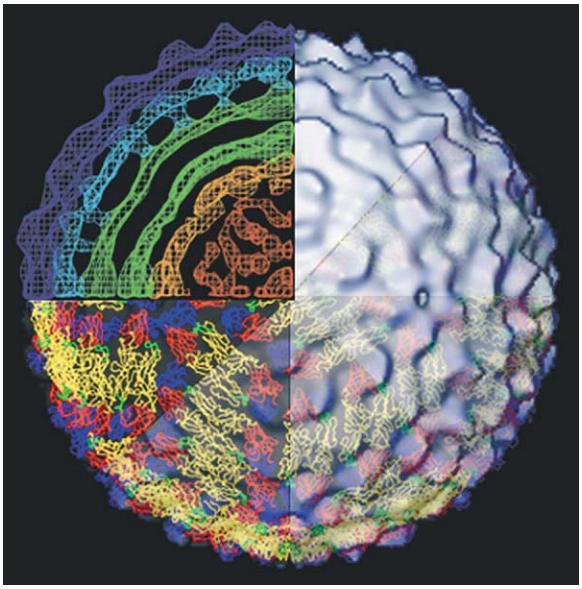

The first structure of a flavivirus has been determined by using a combination of cryoelectron microscopy and fitting of the known structure of glycoprotein E into the electron density map. The virus core, within a lipid bilayer, has a less-ordered structure than the external, icosahedral scaffold of 90 glycoprotein E dimers. The three E monomers per icosahedral asymmetric unit do not have quasiequivalent symmetric environments. Difference maps indicate the location of the small membrane protein M relative to the overlaying scaffold of E dimers. The structure suggests that flaviviruses, and by analogy also alphaviruses, employ a fusion mechanism in which the distal barrels of domain II of the glycoprotein E are inserted into the cellular membrane.

□ **Molecular basis of proton motive force generation: structure of formate dehydrogenase-N.** Mika Jormakka, Susanna Törnroth, Bernadette Byrne, and So Iwata (2002). Science *295*, 1863–1868.

The structure of the membrane protein formate dehydrogenase-N (Fdn-N), a major component of *Escherichia coli* nitrate respiration, has been determined at 1.6 Å. The structure demonstrates 11 redox centers, including molybdopterin-guanine dinucleotides, five [4Fe-4S] clusters, two heme b groups, and a menaquinone analog. These redox centers are aligned in a single chain, which extends almost 90 angstroms through the enzyme. The menaquinone reduction site associated with a possible proton pathway was also characterized. This structure provides critical insights into the proton motive force generation by redox loop, a common mechanism among a wide range of respiratory enzymes.

□ **Structure of a cofactor-deficient nitrogenase MoFe protein**. Benedikt Schmid, Markus W. Ribbe, Oliver Einsle, Mika Yoshida, Leonard M. Thomas, Dennis R. Dean, Douglas C. Rees, and Barbara K. Burgess (2002). Science *296*, 352–356.

One of the most complex biosynthetic processes in metallobiochemistry is the assembly of nitrogenase, the key enzyme in biological nitrogen fixation. The authors describe the crystal structure of an iron-molybdenum cofactor-deficient form of the nitrogenase MoFe protein, into which the cofactor is inserted in the final step of MoFe protein assembly. The MoFe protein folds as a heterotetramer containing two copies each of the homologous and subunits. In this structure, one of the three subunit domains exhibits a substantially changed conformation, whereas the rest of the protein remains essentially unchanged. A predominantly positively charged funnel is revealed; this funnel is of sufficient size to accommodate insertion of the negatively charged cofactor.

□ **Crystal structure of the extracellular segment of integrin V3 in complex with an Arg-Gly-Asp ligand**. Jian-Ping Xiong, Thilo Stehle, Rongguang Zhang, Andrzej Joachimiak, Matthias Frech, Simon L. Goodman, and M. Amin Arnaout (2002). Science *296*, 151–155.

The structural basis for the divalent cation-dependent binding of heterodimeric integrins to their ligands, which contain the prototypical Arg-Gly-Asp sequence, is unknown. Interaction with ligands triggers tertiary and quaternary structural rearrangements in integrins that are needed for cell signaling. The authors report the crystal structure of the extracellular segment of integrin V3 in complex with a cyclic peptide presenting the Arg-Gly-Asp sequence. The ligand binds at the major interface between the V and 3 subunits and makes extensive contacts with both. Both tertiary and quaternary changes are observed in the presence of ligand. The tertiary rearrangements take place in A, the ligand binding domain of 3 and ligand binding induces small changes in the orientation of V relative to 3.

□ **Structural basis of gating by the outer membrane transporter FecA**. Andrew D. Ferguson, Ranjan Chakraborty, Barbara S. Smith, Lothar Esser, Dick van der Helm, and Johann Deisenhofer (2002). Science *295*, 1715–1721.

Siderophore-mediated acquisition systems facilitate iron uptake. The authors present the crystallographic structure of the integral outer membrane receptor FecA from *Escherichia coli* with and without ferric citrate at 2.5 and 2.0 Å resolution. FecA is composed of three distinct domains: the barrel, plug, and NH2-terminal extension. Binding of ferric citrate triggers a conformational change of the extracellular loops that close the external pocket of FecA. Ligand-induced allosteric transitions are propagated through the outer membrane by the plug domain, signaling the occupancy of the receptor in the periplasm. These data establish the structural basis of gating for receptors dependent on the cytoplasmic membrane protein TonB.

□ **The structure of the Dead ringer-DNA complex reveals how AT-rich interaction domains (ARIDs) recognize DNA**. Junji Iwahara, Mizuho Iwahara, Gary W. Daughdrill, Joseph Ford, and Robert T. Clubb (2002). EMBO J. *21*, 1197–1209.

The AT-rich interaction domain (ARID) is a DNA binding module found in many eukaryotic transcription factors. The solution structure of an ARID–DNA complex (mol. wt. 25.7 kDa) formed by Dead ringer from *Drosophila melanogaster* reveals that ARIDs recognize DNA through a novel mechanism. This involves major groove immobilization of a large loop that connects the helices of a helix–turn–helix motif, and a structural rearrangement that produces stabilizing contacts from a β-hairpin. Dead ringer's preference for AT-rich DNA arises from three positions within the ARID fold that contact an adenine-thymine base step. The prevalence of serines at all specificity determining positions suggests that ARIDs within SWI/SNF-related complexes will interact with DNA nonsequence specifically.

□ **Structural basis for cooperative DNA binding by two dimers of the multidrug binding protein QacR**. Maria A. Schumacher, Marshall C. Miller, Steve Grkovic, Melissa H. Brown, Ronald A. Skurray, and Richard G. Brennan (2002). EMBO J. *21*, 1210–1218.

The Staphylococcus aureus multidrug binding protein QacR represses transcription of the qacA multidrug transporter gene. QacR is a member of the TetR/CamR family of transcriptional regulators, which share highly homologous N-terminal DNA binding domains connected to non-homologous ligand binding domains. QacR recognizes an unusually long 28 bp operator, IR1, which it binds cooperatively. The crystal structure of a QacR-IR1 complex reveals that the DNA recognition mode of QacR is distinct from TetR, and involves the binding of a pair of QacR dimers. In this unique binding mode, recognition at each IR1 half-site is mediated by a complement of DNA contacts made by two helix-turn-helix motifs. The authors suggest that cooperativity arises from the global undertwisting and major groove widening elicited by the dimer.

□ **Conserved segments 1A and 2B of the intermediate filament dimer: their atomic structures and role in filament assembly**. Sergei V. Strelkov, Harald Herrmann, Norbert Geisler, Tatjana Wedig, Ralf Zimbelmann, Ueli Aebi, and Peter Burkhard (2002). EMBO J. *21*, 1255–1266.

Intermediate filaments (IFs) are key components of the cytoskeleton in higher eukaryotic cells. The elementary IF "building block" is an elongated coiled-coil dimer consisting of four consecutive α-helical segments. The segments 1A and 2B include highly conserved sequences and are critically involved in IF assembly. The

crystal structures of three human vimentin fragments are presented, providing the first insights into the architecture and function of IFs at the atomic level. The fragment corresponding to segment 1A forms a single, amphipatic α-helix, which is compatible with a coiled-coil geometry. While this segment might yield a coiled coil within an isolated dimer, monomeric 1A helices are likely to play a role in specific dimer-dimer interactions during IF assembly. The 2B segment reveals a double-stranded coiled coil, which unwinds near residue Phe351 to accommodate a "stutter". A fragment containing the last seven heptads of 2B interferes heavily with IF assembly and also transforms mature vimentin filaments into a new kind of structure.

☐ **A crystallographic view of interactions between Dbs and Cdc42: PH domain-assisted guanine nucleotide exchange.** Kent L. Rossman, David K. Worthylake, Jason T. Snyder, David P. Siderovski, Sharon L. Campbell, and John Sondek (2002). EMBO J. *21*, 1315–1326.

Dbl-related oncoproteins are guanine nucleotide exchange factors (GEFs) specific for Rho guanosine triphosphatases (GTPases), and invariably possess tandem Dbl (DH) and pleckstrin homology (PH) domains. The crystal structure of a DH/PH fragment from Dbs in complex with Cdc42 is presented. The PH domain is in a unique conformation distinct from that in the related structures of Sos1 and Tiam1·Rac1. It participates with the DH domain in binding Cdc42, primarily through a set of interactions involving switch 2 of the GTPase. Comparative sequence analysis suggests that a subset of Dbl-family proteins will utilize their PH domains similarly to Dbs.

☐ **Crystal structures of two intermediates in the assembly of the papillomavirus replication initiation complex.** Eric J. Enemark, Arne Stenlund, and Leemor Joshua-Tor (2002). EMBO J. *21*, 1487–1496.

Initiation of DNA replication of the papillomavirus genome is a multi-step process involving the sequential loading of viral E1 protein subunits onto the origin of replication. Here the authors have captured structural snapshots of two sequential steps in the assembly process. Initially, an E1 dimer binds to adjacent major grooves on one face of the double helix; a second dimer then binds to another face of the helix. Each E1 monomer has two DNA binding modules: a DNA binding loop, which binds to one DNA strand and a DNA binding helix, which binds to the opposite strand. The nature of DNA binding suggests a mechanism for the transition between double- and single-stranded DNA binding that is implicit in the progression to a functional helicase.

☐ **The crystal structure of *Helicobacter pylori* cysteine-rich protein B reveals a novel fold for a penicillin binding protein.** Lucas Lüthy, Markus G. Grütter, and Peer R. E. Mittl (2002). J. Biol. Chem. *277*, 10187–10193.

Colonization of the gastric mucosa with the spiral-shaped proteobacterium *Helicobacter pylori* is probably the most common chronic infection in humans. The crystal structure of H. pylori cysteine-rich protein (Hcp) B reveals a modular architecture consisting of four α/α-motifs that are cross-linked by disulfide bridges. In contrast to the related tetratricopeptide repeat, the Hcp repeat is 36 amino acids long. HcpB is capable of binding and hydrolyzing 6-amino penicillinic acid and 7-amino cephalosporanic acid derivatives. The HcpB fold is distinct from the fold of any known penicillin binding protein. The putative penicillin binding site is located in an amphipathic groove on the concave side of the molecule.

☐ **Multi-resolution contour-based fitting of macromolecular structures.** Pablo Chacón and Willy Wriggers (2002). J. Mol. Biol. *317*, 375–384.

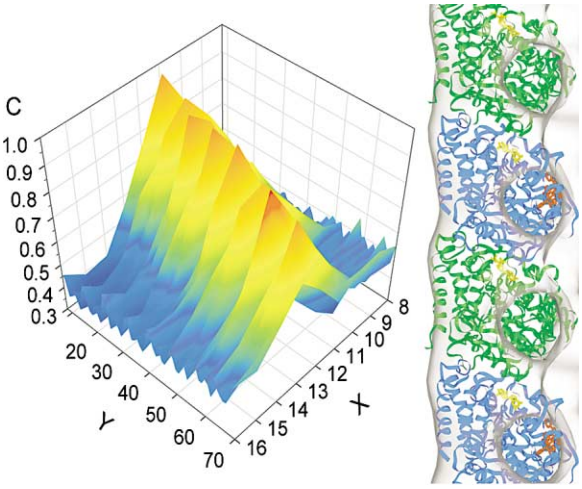

A novel contour-based matching criterion is presented for the quantitative docking of high-resolution structures of components into low-resolution maps of macromolecular complexes. The proposed Laplacian filter is combined with a six-dimensional search using fast Fourier transforms to rapidly scan the rigid-body degrees of freedom of a probe molecule relative to a fixed target density map. A comparison of the docking performance with the standard cross-correlation criterion demonstrates that contour matching with the Laplacian filter significantly extends the viable resolution range of correlation-based fitting to resolutions as low as 30 Å. As an example, a new pseudo-atomic model of a microtubule was constructed from a 20 Å resolution EM map and from atomic structures of α- and β-tubulin subunits (see figure).

☐ **Structural milestones in the reaction pathway of an amide hydrolase: substrate, acyl, and product complexes of cephalothin with AmpC β-lactamase.** Beth M. Beadle, Indi Trehan, Pamela J. Focia, and Brian K. Shoichet (2002). Structure *10*, 413–424.

β-lactamases hydrolyze β-lactam antibiotics and are the leading cause of bacterial resistance to these drugs.

Although β-lactamases have been extensively studied, structures of the substrate-enzyme and product-enzyme complexes have proven elusive. Here, the structure of a mutant AmpC in complex with the β-lactam cephalothin in its substrate and product forms was determined by X-ray crystallography to 1.53 Å resolution. The acyl-enzyme intermediate between AmpC and cephalothin was determined to 2.06 Å resolution. The ligand undergoes a dramatic conformational change as the reaction progresses, with the characteristic six-membered dihydrothiazine ring of cephalothin rotating by 109°. These structures correspond to all three intermediates along the reaction path and provide insight into substrate recognition, catalysis, and product expulsion.

□ **Structural determinants for GoLoco-induced inhibition of nucleotide release by G subunits.** Randall J. Kimple, Michelle E. Kimple, Laurie Betts, John Sondek, and David P. Siderovski (2002). Nature *416*, 878–881.

Heterotrimeric G-proteins bind to cell-surface receptors and are required for the transmission of many signals from outside the cell. Upon activation of the Gα subunit by binding of GTP, the Gα and Gβγ subunits dissociate and interact with effector proteins for signal transduction. Regulatory proteins with the 19-amino-acid GoLoco motif can bind to Gα subunits and maintain G protein subunit dissociation in the absence of Gα activation. The authors determined the crystal structure of Gαi1–GDP bound to the GoLoco region of the "regulator of G protein signaling" protein RGS14. Key contacts are described between the GoLoco motif and Gα protein, including the extension of GoLoco's conserved Asp/Glu-Gln-Arg triad into the nucleotide binding pocket of Gα to make direct contact with the GDP α- and β-phosphates. The Gα all-helical domain and GoLoco-region carboxy-terminal region appear to control specificity.

□ **Structure of the Cul1-Rbx1-Skp1-F boxSkp2 SCF ubiquitin ligase complex**. Ning Zheng, Brenda A. Schulman, Langzhou Song, Julie J. Miller, Philip D. Jeffrey, Ping Wang, Claire Chu, Deanna M. Koepp, Stephen J. Elledge, Michele Pagano, Ronald C. Conaway, Joan W. Conaway, J. Wade Harper, and Nikola P. Pavletich (2002). Nature *416*, 703–709.

SCF complexes are the largest family of E3 ubiquitin-protein ligases and mediate the ubiquitination of diverse regulatory and signaling proteins. The crystal structure of the Cul1-Rbx1-Skp1-F boxSkp2 SCF complex shows that Cul1 is an elongated protein that consists of a long stalk and a globular domain. The globular domain binds the RING finger protein Rbx1 through an intermolecular β sheet, forming a two-subunit catalytic core that recruits the ubiquitin-conjugating enzyme. The long stalk, which consists of three repeats of a novel five-helix motif, binds the Skp1-F boxSkp2 protein substrate-recognition complex at its tip. Cul1 serves as a rigid scaffold that organizes the Skp1-F boxSkp2 and Rbx1 subunits, holding them over 100 Å apart. The structure suggests that Cul1 may contribute to catalysis through the positioning of the substrate and the ubiquitin-conjugating enzyme.

□ **Structure of the RPA trimerization core and its role in the multistep DNA binding mechanism of RPA (2002).** Elena Bochkareva, Sergey Korolev, Susan P. Lees-Miller, and Alexey Bochkarev (2002). EMBO J. *21*, 1855–1863.

The human single-stranded DNA binding protein, replication protein A (RPA) binds DNA in at least two different modes: initial [8–10 nucleotides (nt)] and stable (30 nt). Switching from 8 to 30 nt mode is associated with a large conformational change. The authors describe the crystal structure of the RPA trimerization core, comprising the C-terminal DNA binding domain of subunit RPA70 (DBD-C), the central DNA binding domain of subunit RPA32 (DBD-D) and the entire RPA14 subunit. All three domains are built around a central oligonucleotide/oligosaccharide binding (OB)-fold and flanked by a helix at the C terminus. Trimerization is mediated by three C-terminal helices arranged in parallel. The OB-fold of DBD-C possesses unique structural features: embedded zinc ribbon and helix-turn-helix motifs. Structural and functional data indicate that switching from 8–10 to 30 nt mode is mediated by DNA binding with the trimerization core.

□ **Structure of the carboxyl-terminal Src kinase, Csk.** Akira Ogawa, Yoshiharu Takayama, Hiroaki Sakai, Khoon Tee Chong, Satoru Takeuchi, Atsushi Nakagawa, Shigeyuki Nada, Masato Okada, and Tomitake Tsukihara (2002). J. Biol. Chem. *277*, 14351–14354.

The carboxyl-terminal Src kinase (Csk) is a negative regulator for the Src family tyrosine kinases (SFKs) that play pivotal roles in cell signaling. The authors describe the crystal structure of full-length Csk. The asymmetric unit contains six molecules that can be classified as active or inactive states according to the coordinations of catalytic residues. Csk assembles the SH2 and SH3 domains differently from inactive SFKs, and their binding pockets are oriented outward enabling intermolecular interactions. In active molecules, the SH2-kinase and SH2-SH3 linkers are tightly stuck to the N-lobe of the kinase domain to stabilize the active conformation, and there is a direct linkage between the SH2 and the kinase domains. In inactive molecules, the SH2 domains are rotated, destroying the linkage to the kinase domain. These observations suggest that Csk can be regulated through coupling of the SH2 and kinase domains and that Csk provides a novel built-in activation mechanism for cytoplasmic tyrosine kinases.

□ **Structure of two iron binding proteins from *Bacillus anthracis*.** Elena Papinutto, William G. Dundon, Nea Pitulis, Roberto Battistutta, Cesare Montecucco, and Giuseppe Zanotti (2002). J. Biol. Chem. *277*, 15093–15098.

Bacillus anthracis is currently under intense investigation due to its potential as a human pathogen. A novel class of immunogenic bacterial proteins consists of dodecamers homologous to the DNA binding protein of *Escherichia coli* (Dps). Two Dps homologous genes are present in the *B. anthracis* genome. The crystal structures of these two proteins (Dlp-1 and Dlp-2) have been determined and are presented here. They are sphere-like proteins with an internal cavity. The authors show that they act as ferritins and are involved in iron uptake and regulation, a fundamental function during bacterial growth.

Chosen by **Robert Liddington,[1] Christin Frederick,[2] Stephen D. Fuller,[3] and Sophie Jackson[4]**
[1]Program on Cell Adhesion
The Burnham Institute
10901 North Torrey Pines Road
La Jolla, California 92037
[2]Laboratory of X-Ray Crystallography
Dana-Farber Cancer Institute
44 Binney Street
Boston, Massachusetts 02115
[3]Division of Structural Biology
Wellcome Trust Centre for Human Genetics
Henry Wellcome Building for Genomic Medicine
Roosevelt Drive
Headington, Oxford
OX3 7BN
United Kingdom
[4]Department of Chemistry
University of Cambridge
Lensfield Road
Cambridge CB2 1EW
United Kingdom